Supporting Information

Excessive force-induced root resorption depends on macrophage YAP activation

Liyuan Chen[1,2#], Shuyue Zhu[1#], Wei Wang[3], Zimo Zhao[1], Huajie Yu[2], Boyang Zhang[3], Shiying Zhang[1], Yuwei Liu[3], Zhuowen Gu[1], Danqing He[1*], Yan Liu[1*]

[1]Department of Orthodontics, Central Laboratory, Peking University School and Hospital for Stomatology & National Center for Stomatology & National Clinical Research Center for Oral Diseases & National Engineering Research Center of Oral Biomaterials and Digital Medical Devices & Beijing Key Laboratory of Digital Stomatology & Research Center of Engineering and Technology for Computerized Dentistry Ministry of Health & NMPA Key Laboratory for Dental Materials, Beijing 100081, China.

[2]Peking University Hospital of Stomatology Fourth Division, Beijing, China.

[3]Department of Immunology, School of Basic Medical Sciences, NHC Key Laboratory of Medical Immunology, Medicine Innovation Center for Fundamental Research on Major Immunology-related Diseases, Peking University, Beijing, China.

[#]These authors contributed equally:Liyuan Chen, Shuyue Zhu.

*Corresponding author. Email: orthoyan@bjmu.edu.cn (Y.L.), hedanqing@bjmu.edu.cn (D.H.)

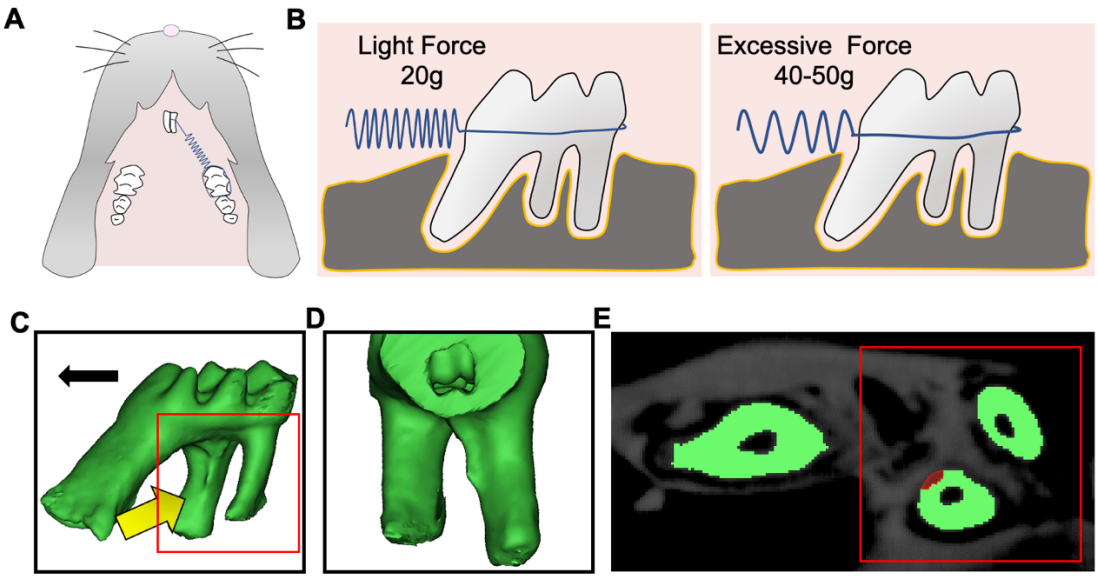

Supplementary Fig. S1 Establishment and evaluation of the orthodontic force model. A. Schematic illustration of mechanical force application to the maxillary first molar in occlusal view. B. Schematic illustration of the orthodontic force-loading model. Approximately 20 g was used as the light-force condition, whereas 40–50 g was used as the excessive-force condition. C. Representative micro-CT images of the maxillary first molars. The arrow indicates the viewing direction, and the red box indicates the region of interest. D. Magnified micro-CT images of the distal roots of the maxillary first molars. E. Three-dimensional segmentation of the distal roots, with root resorption areas shown in red.

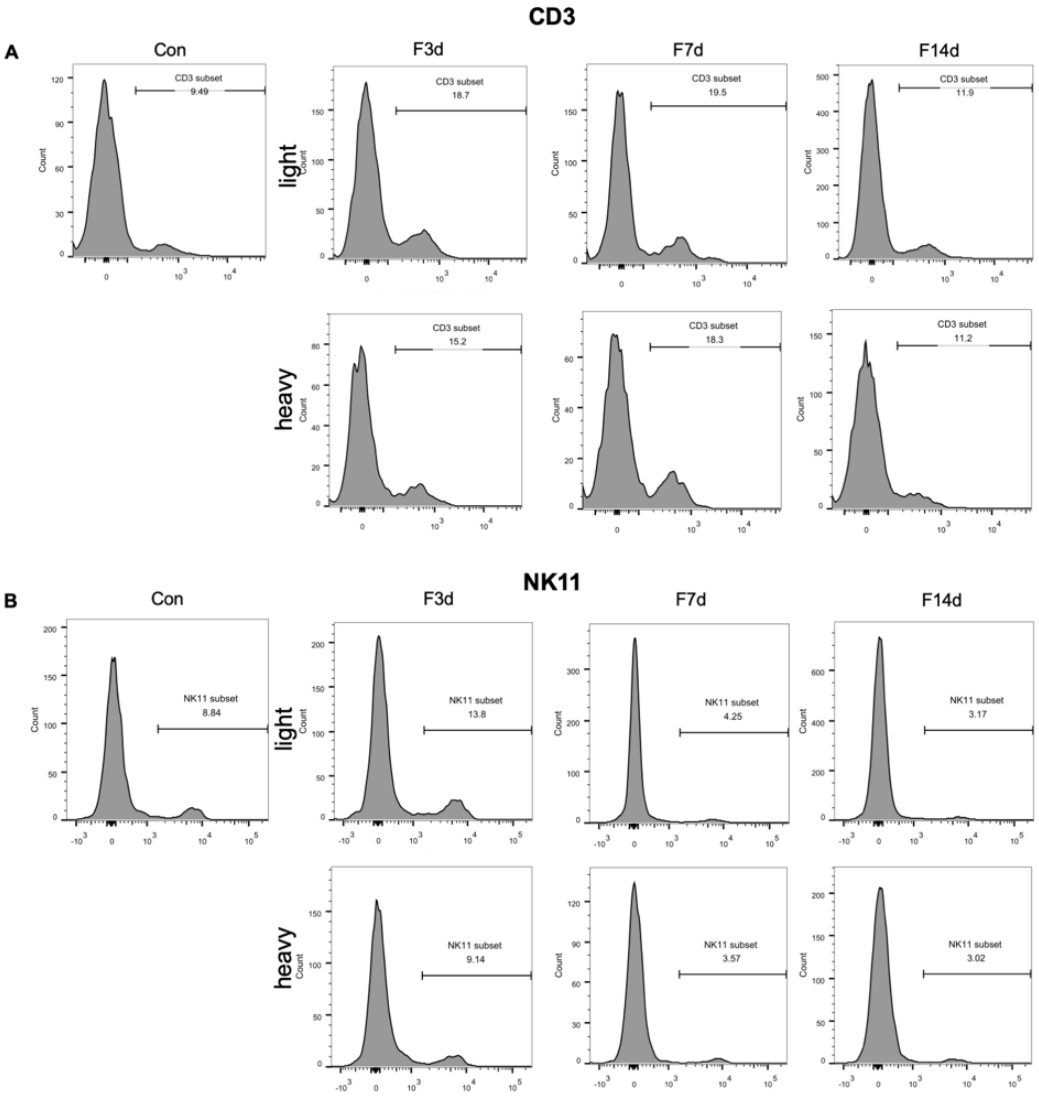

Supplementary Fig. S2 Representative flow cytometry plots showing $CD3^+$ T lymphocytes (A) and $NK1.1^+$ NK cells (B) in periodontal tissues following mechanical force loading.

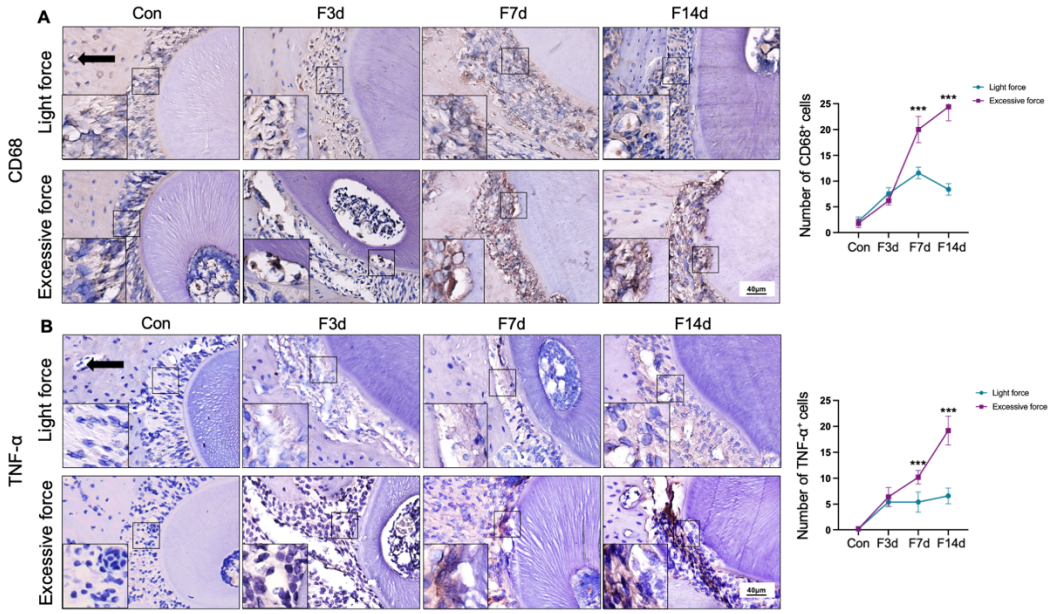

Supplementary Fig. S3 A. Representative immunohistochemical staining images of the macrophage-related proteins CD68 in the compression side of distobuccal roots were detected. B. Representative immunohistochemical staining images of the inflammation-related protein TNF-α in the compression side of distobuccal roots were detected. Large boxed areas show high magnification views of the small boxed areas. The arrow represents the direction of force application. Scale bar: 40 μm. $n = 5$; ***P < 0.001 versus Con.

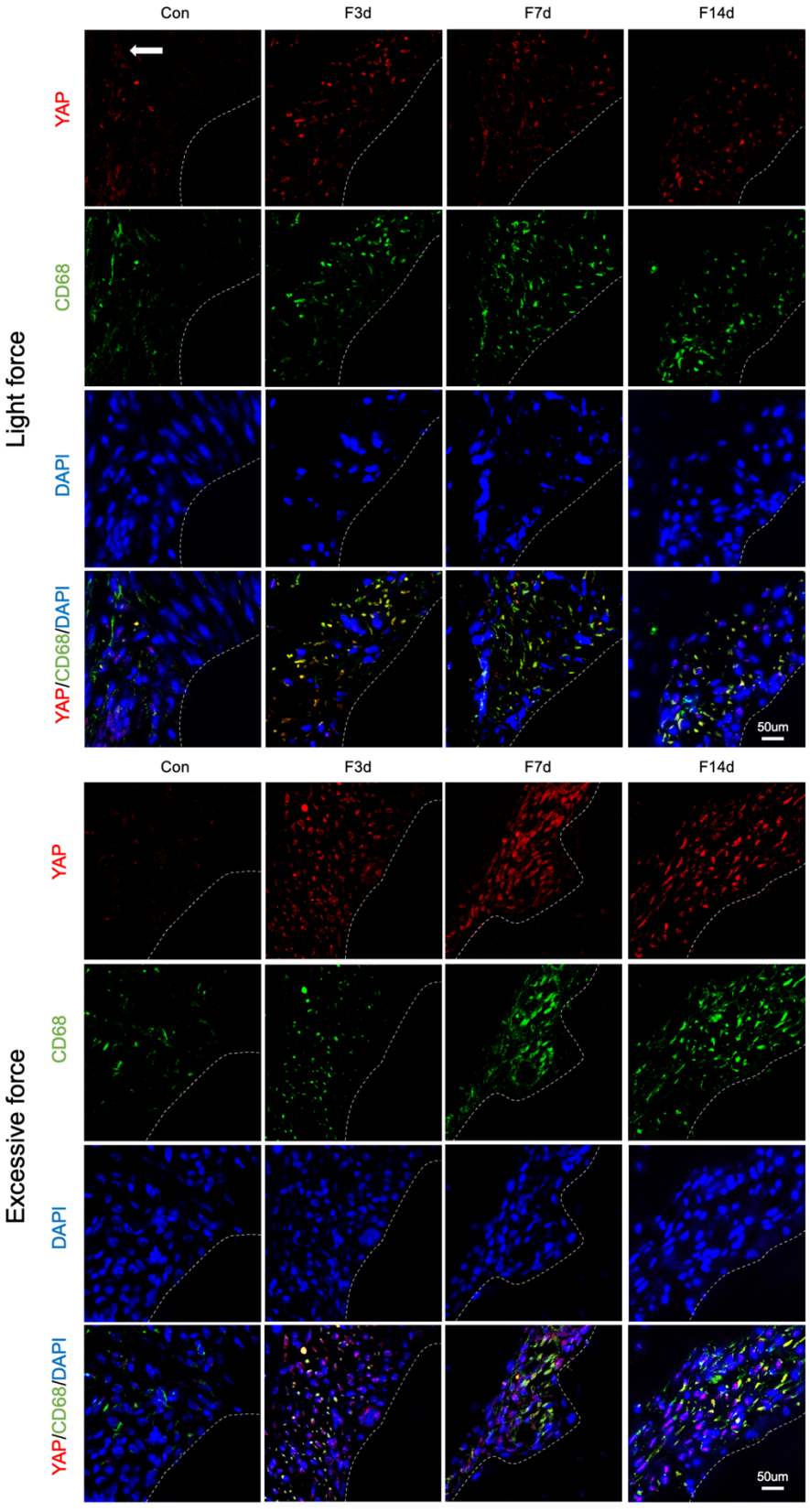
Con
F3d
F7d
F14d
Light force
YAP
CD68
DAPI
YAP/CD68/DAPI
50um
Con
F3d
F7d
F14d
Excessive force
YAP
CD68
DAPI
YAP/CD68/DAPI
50um

46

Supplementary Fig. S4 Representative immunofluorescence images of Fig. 1D. Dashed lines mark the outline of distobuccal roots. n = 5. The arrow represents the direction of force application.

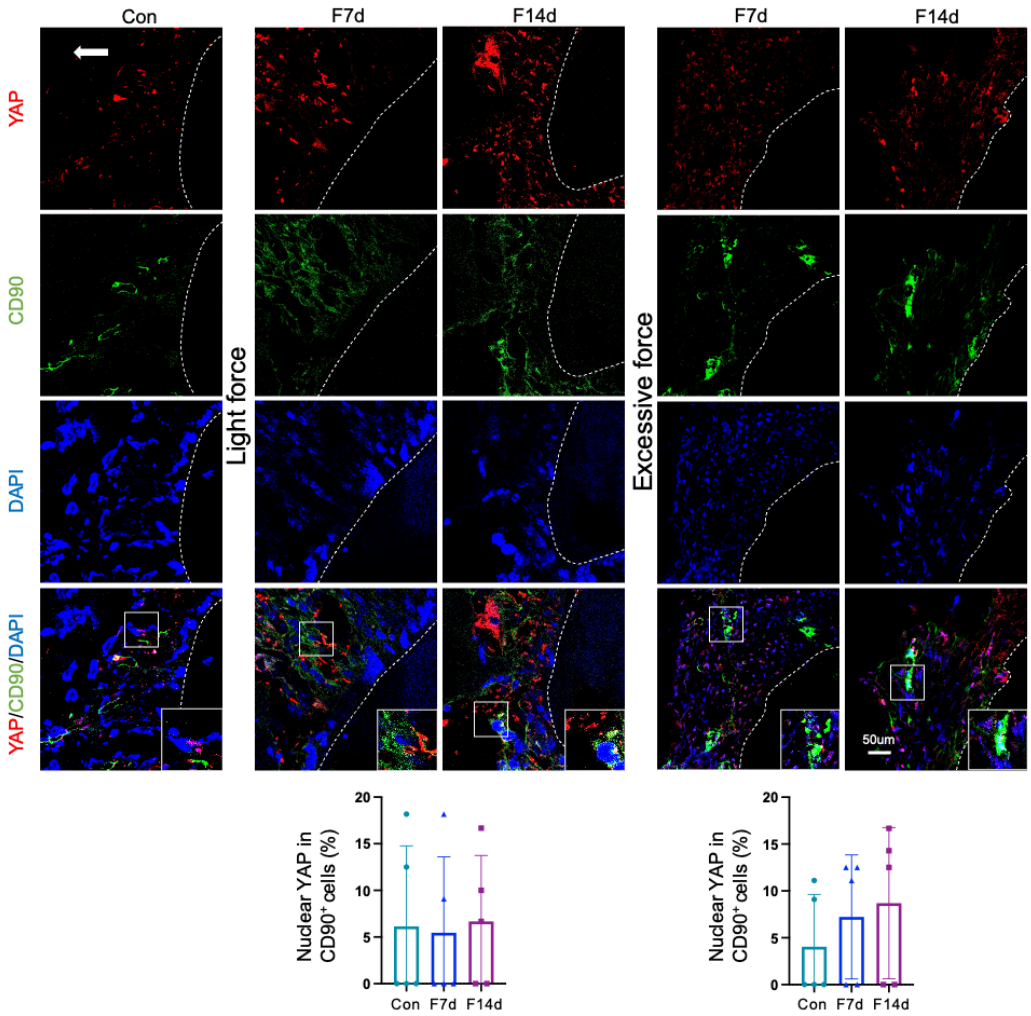

Supplementary Fig. S5 Representative immunofluorescence images on the compression side of distobuccal roots. Dashed lines mark the outline of distobuccal roots. Large boxed areas show high-magnification views of the small boxed areas. Scale bar: 50 μm. n = 5. The arrow represents the direction of force application.

A

Yap1-loxp	F1: 5'-GGGAAACTGGTACTTACTAGGTGAA-3' R1: 5'-GCTTAATCTTCACAAAGGGGTAGT-3'
Lyz2-Cre-MT	Lyz2-Cre-MF : 5'-CCCAGAAATGCCAGATTACG-3' Lyz2-Cre-MR : 5'-CTTGGGCTGCCAGAATTTCTC-3'
Lyz2-Cre-WT	Lyz2-Cre-WR: 5'-TTACAGTCGGCCAGGCTGAC-3' Lyz2-Cre-MR: 5'-CTTGGGCTGCCAGAATTTCTC-3'
Marker	Yap1-loxp (MT: 283 bp, WT: 222 bp)

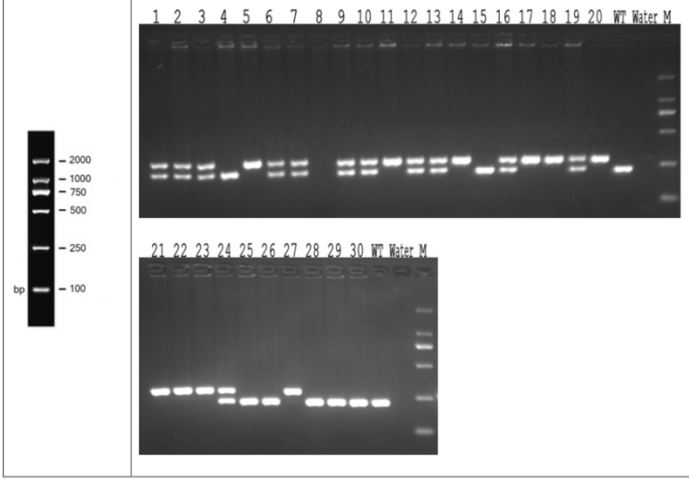

B

Marker	Lyz2-Cre-MT (MT: 721 bp)

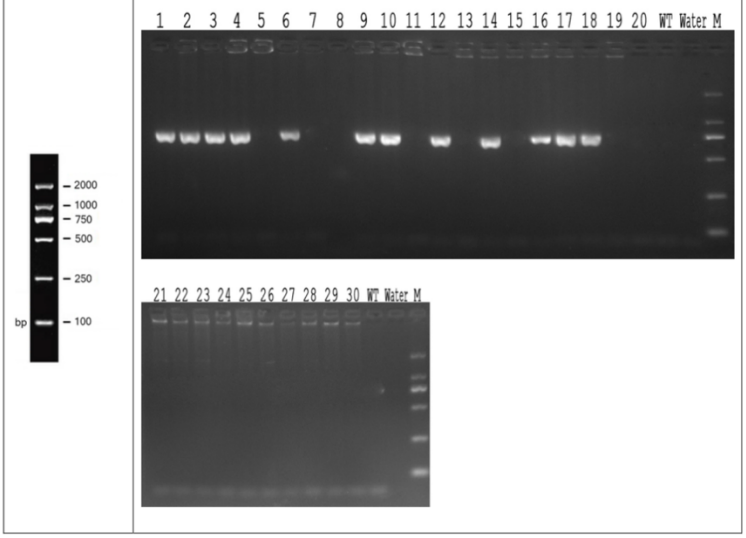

Marker	Lyz2-Cre-WT (WT: 346 bp)

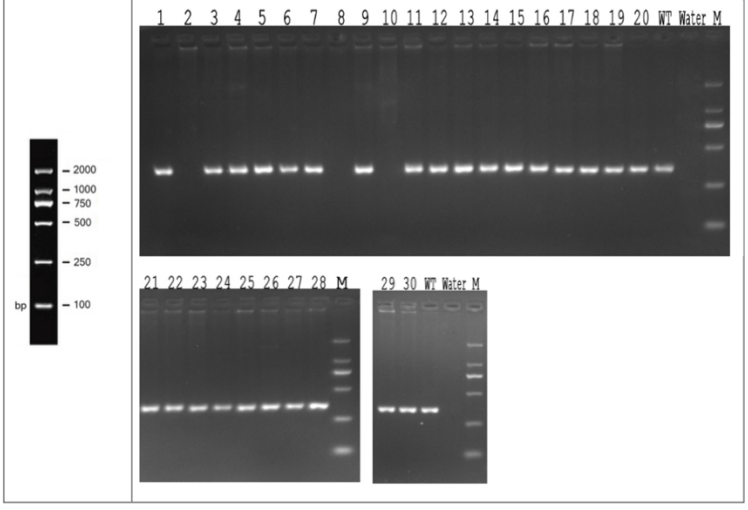

Supplementary Fig. S6 Representative PCR genotyping results for *Yap1*$^{flox/flox}$; *Lyz2*-Cre mice and *Yap1*$^{flox/flox}$ controls. A. *Yap1*-loxp genotyping showing mutant and wild-type bands at 283 bp and 222 bp, respectively. B. *Lyz2*-Cre genotyping showing mutant and wild-type bands at 721 bp and 346 bp, respectively. M, DNA marker; Water, negative control; MT, mutant; WT, wild type.

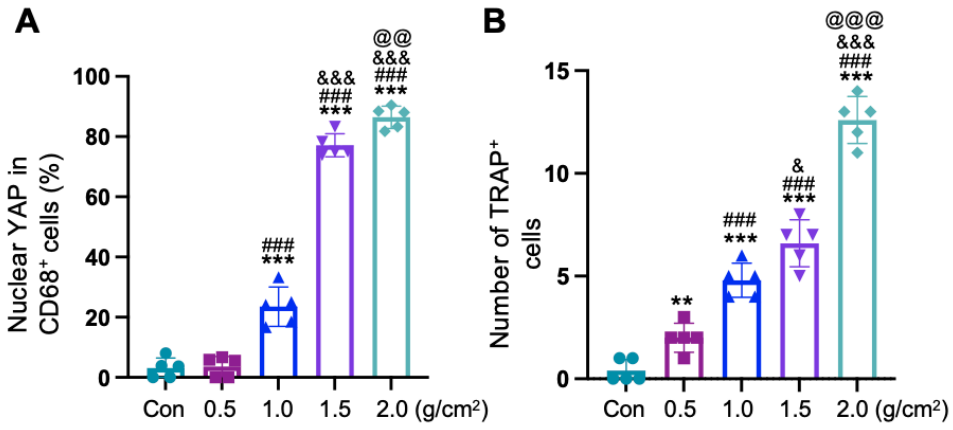

Supplementary Fig. S7 A. Quantification of Fig. 3H (Immunofluorescence images of nuclear YAP in CD68$^+$ cells under different force loading for 24 h *in vitro*). $n = 5$. ***P < 0.001 versus Con; ###P < 0.001 versus 0.5g/cm^2; &&&P < 0.001 versus 1.0g/cm^2, @@ P < 0.01 versus 1.5g/cm^2. B. Statistical results of Fig. 3J (images of TRAP staining of RAW264.7 after odontoclast/osteoclast induction). $n = 5$. **P < 0.01, ***P < 0.001 versus Con; #P < 0.05, ###P < 0.001 versus 0.5g/cm^2; &P < 0.05, &&&P < 0.001 versus 1.0g/cm^2, @@ P < 0.01 versus 1.5g/cm^2.

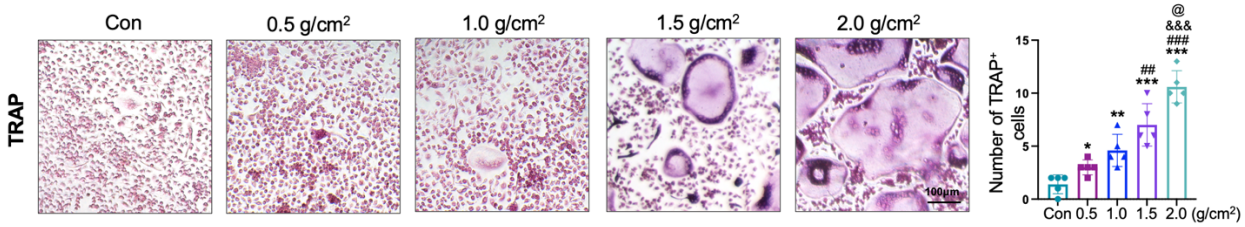

Supplementary Fig. S8 Representative images of TRAP staining of BMMs after odontoclast/osteoclast induction by M-CSF and RANKL. Scale bar: 100 μm. $n = 5$. *P < 0.05, **P < 0.01, ***P < 0.001 versus Con; ##P < 0.01, ###P < 0.001 versus 0.5g/cm^2; &&&P < 0.001 versus 1.0g/cm^2, @ P < 0.05 versus 1.5g/cm^2.

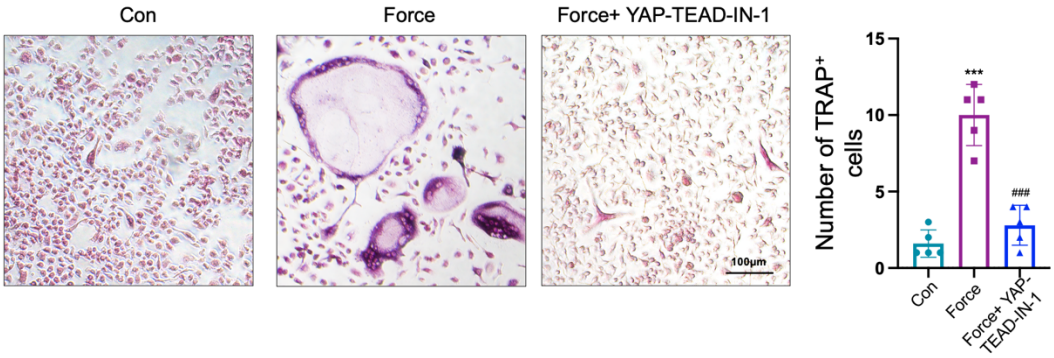

Supplementary Fig. S9 Representative TRAP-staining images and quantification of BMM-derived odontoclasts/osteoclasts following excessive compressive force with or without YAP-TEAD-IN-1 treatment. Scale bar: 100 μm. $n = 5$. ***P < 0.001 versus Con; ###P < 0.001 versus Force.

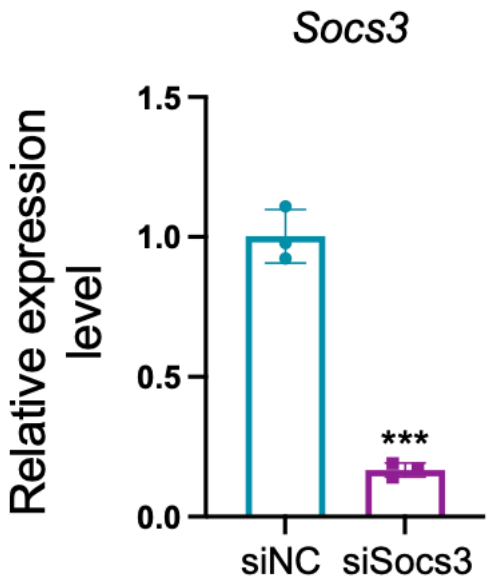

Supplementary Fig. S10 qPCR validation of *Socs3* knockdown efficiency in RAW264.7 cells following siSOCS3 transfection. $n = 3$. ***P < 0.001 versus siNC.

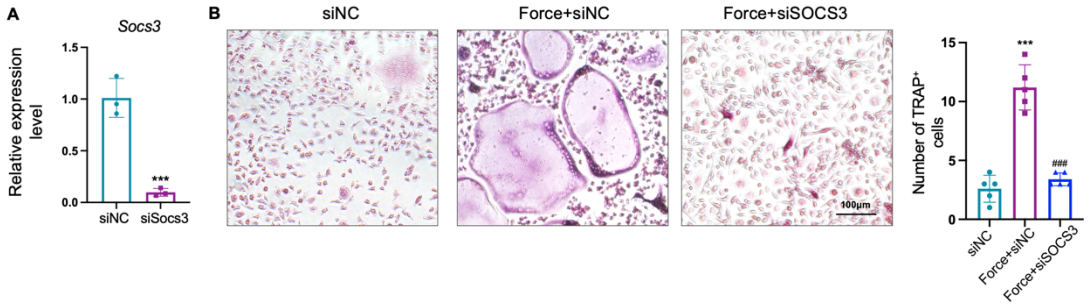

86

87 **Supplementary Fig. S11** A. Effects of *SOCS3* knockdown on BMM
88 odontoclast/osteoclast differentiation. n = 3. ***P < 0.001 versus siNC. B.
89 Representative images of TRAP staining of BMMs after odontoclast/osteoclast
90 induction by M-CSF and RANKL. Scale bar: 100 μm. n = 5. ***P < 0.001 versus siNC;
91 ###P < 0.001 versus Force+siNC.

92

Fig. 3E

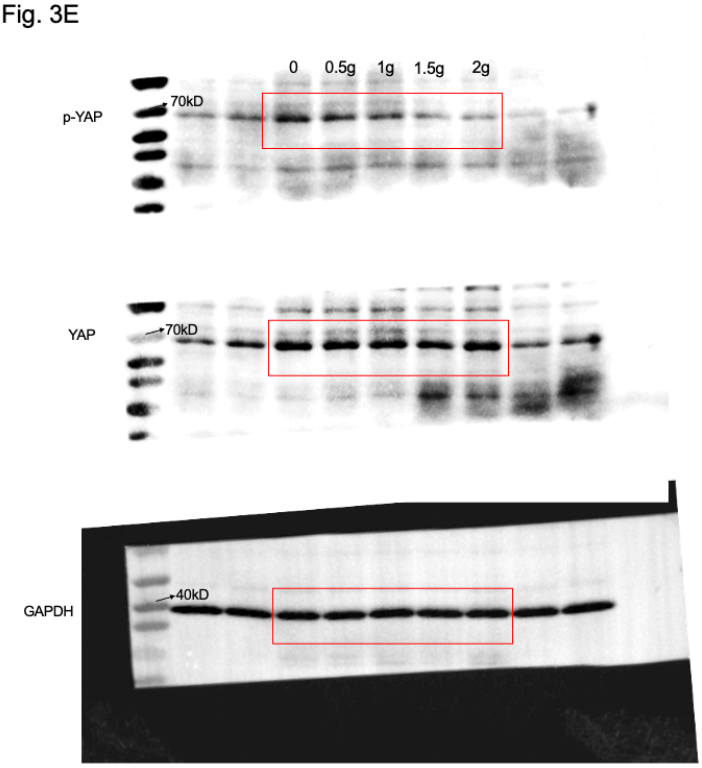

Fig. 3F, G

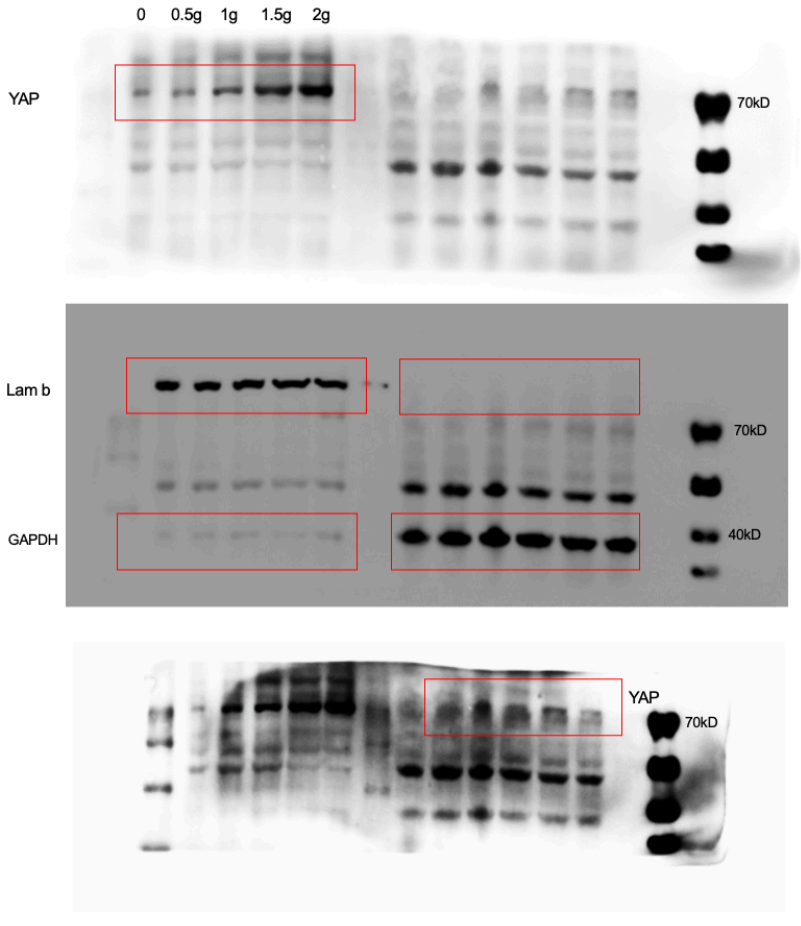

93

Supplementary Fig. S12 Uncropped Western blot images corresponding to Fig. 3E–G.